

## Electron Transport Properties of Atomic Carbon Nanowires between Graphene Electrodes

Lei Shen,<sup>†,‡,||</sup> Minggang Zeng,<sup>†,¶,||</sup> Shuo-Wang Yang,<sup>\*,‡</sup> Chun Zhang,<sup>†</sup>  
Xuefeng Wang,<sup>§</sup> and Yuanping Feng<sup>\*,†</sup>

Department of Physics, 2 Science Drive 3, National University of Singapore, Singapore 117542, Singapore, Institute of High Performance Computing, 1 Fusionopolis Way, 16-16 Connexis, Singapore 138632, Singapore, NanoCore, 5A Engineering Drive 4, National University of Singapore, Singapore 117576, Singapore, and Department of Physics, Soochow University, Suzhou 215006, China

Received November 10, 2009; E-mail: yangsw@ihpc.a-star.edu.sg; phyfyp@nus.edu.sg

**Abstract:** Long, stable, and free-standing linear atomic carbon wires (carbon chains) have been carved out from graphene recently [Meyer et al. *Nature (London)* **2008**, *454*, 319; Jin et al. *Phys. Rev. Lett.* **2009**, *102*, 205501]. They can be considered as extremely narrow graphene nanoribbons or extremely thin carbon nanotubes. It might even be possible to make use of high-strength and identical (without chirality) carbon wires as a transport channel or on-chip interconnects for field-effect transistors. Here we investigate electron transport properties of linear atomic carbon wire–graphene junctions by combining nonequilibrium Green's function with density functional theory. For short wires, linear ballistic transport is observed in wires consisting of odd numbers of carbon atoms but not in those consisting of even numbers of carbon atoms. For wires longer than 2.1 nm as fabricated above, however, the ballistic conductance of carbon wire–graphene junctions is independent of the structural distortion, structural imperfections, and hydrogen impurity adsorbed on the linear carbon wires, except for oxygen impurity adsorption under a low bias. As such, the epoxy groups might be the origin of experimentally observed low conductance in the carbon chain. Moreover, double-atomic carbon chains exhibit a negative differential resistance effect.

### Introduction

Compared with silicon nanowires (SiNWs), which have been utilized in many practical device applications<sup>1</sup> with considerable theoretical support,<sup>2</sup> carbon nanowires (CNWs) have attracted less attention due to the limited synthetic and fabrication technologies.<sup>3,4</sup> Recently, two research groups have successfully carved out linear atomic carbon wires (carbon chains) from

graphene by using a high-energy electron beam.<sup>5–7</sup> These carbon chains are longer and more stable than those previously synthesized using other methods.<sup>3,4</sup> From an experimental point of view, this method avoids the difficulty of transferring carbon wires to substrates and coating metallic electrodes because their parent, graphene, is already on a substrate and can be used as an electrode directly.<sup>8</sup> Recently, graphene nanoribbons (GNRs) have shown promise for future generations of transistors.<sup>9–19</sup>

<sup>†</sup> Department of Physics, National University of Singapore.

<sup>‡</sup> Institute of High Performance Computing.

<sup>¶</sup> NanoCore, National University of Singapore.

<sup>§</sup> Soochow University.

<sup>||</sup> These authors contributed equally to this work.

- (1) (a) Cui, Y.; Wei, Q.; Park, H.; Lieber, C. M. *Science* **2001**, *293*, 1289. (b) Hahm, J.; Lieber, C. M. *Nano Lett.* **2004**, *4*, 51. (c) Cui, Y.; Lieber, C. M. *Science* **2001**, *291*, 851. (d) Tian, B.; Zheng, X.; Kempa, T. J.; Fang, Y.; Yu, N.; Yu, G.; Huang, J.; Lieber, C. M. *Nature* **2007**, *449*, 885.
- (2) (a) Ng, M.-F.; Shen, L.; Zhou, L.; Yang, S.-W.; Tan, V. B. C. *Nano Lett.* **2008**, *11*, 3662. (b) Yao, D. L.; Zhang, G.; Li, B. W. *Nano Lett.* **2008**, *12*, 4557. (c) Yang, N.; Zhang, G.; Li, B. W. *Nano Lett.* **2008**, *1*, 276. (d) Fagas, G.; Greer, J. C. *Nano Lett.* **2009**, *5*, 1856.
- (3) (a) Derycke, V.; Soukiassian, P.; Mayne, A.; Dujardin, G.; Gautier, J. *Phys. Rev. Lett.* **1998**, *81*, 5869. (b) Zhao, X.; Ando, Y.; Liu, Y.; Jinno, M.; Suzuki, T. *Phys. Rev. Lett.* **2003**, *90*, 187401. (c) Rusznyak, A.; Zolyomi, V.; Kurti, J.; Yang, S.; Kertesz, M. *Phys. Rev. B* **2005**, *72*, 155420. (d) Baughman, R. H. *Science* **2006**, *312*, 1009.
- (4) (a) Yuzvinsky, T. D.; Mickelson, W.; Aloni, S.; Begtrup, G. E.; Kis, A.; Zettl, A. *Nano Lett.* **2006**, *6*, 2718. (b) Troiani, H. E.; Miki-Yoshida, M.; Camacho-Bragado, G. A.; Marques, M. A. L.; Rubio, A.; Ascencio, J. A.; Jose-Yacamán, M. *Nano Lett.* **2003**, *6*, 751.

- (5) Meyer, J. C.; Girit, C. O.; Crommie, M. F.; Zettl, A. *Nature* **2008**, *454*, 319.
- (6) Chuvilin, A.; Meyer, J. C.; Algara-Siller, G.; Kaiser, U. *New J. Phys.* **2009**, *11*, 083019.
- (7) Jin, C.; Lan, H.; Peng, L.; Suenaga, K.; Iijima, S. *Phys. Rev. Lett.* **2009**, *102*, 205501.
- (8) Koleini, M.; Paulsson, M.; Brandbyge, M. *Phys. Rev. Lett.* **2007**, *98*, 197202.
- (9) (a) Fujita, M.; Wakabayashi, K.; Nakada, K.; Kusakabe, K. *J. Phys. Soc. Jpn.* **1996**, *65*, 1920. (b) Nakada, K.; Fujita, M.; Dresselhaus, G.; Dresselhaus, M. *Phys. Rev. B* **1996**, *54*, 17954.
- (10) Cancado, L.; Pimenta, M.; Neves, B.; Medeiros-Ribeiro, G.; Enoki, T.; Kobayashi, Y.; Takai, K.; Fukui, K.; Dresselhaus, M.; Saito, R.; Jorio, A. *Phys. Rev. Lett.* **2004**, *93*, 047403.
- (11) Neto, A. H. C.; Guinea, F.; Peres, N. M. R.; Novoselov, K. S.; Geim, A. K. *Rev. Mod. Phys.* **2009**, *81*, 109.
- (12) Geim, A. K.; Novoselov, K. S. *Nat. Mater.* **2007**, *6*, 183.
- (13) Han, M. Y.; Ozyilmaz, B.; Zhang, Y. B.; Kim, P. *Phys. Rev. Lett.* **2007**, *98*, 206805.
- (14) Son, Y.-W.; Cohen, M. L.; Louie, S. G. *Phys. Rev. Lett.* **2006**, *97*, 216803.
- (15) Peres, N. M. R.; Neto, A. H. C.; Guinea, F. *Phys. Rev. B* **2006**, *73*, 195411.
- (16) Wang, X. R.; Ouyang, Y. J.; Li, X. L.; Wang, H. L.; Guo, J.; Dai, H. J. *Phys. Rev. Lett.* **2008**, *10*, 206803.

However, research on GNRs is still in the early stage, in part because two challenges currently hamper the practical application of GNRs in field-effect transistors (FETs). One is the difficulty in getting sub-10-nm width semiconducting GNRs, due to the limitation of the current lithography technique.<sup>16,17</sup> The other is the chirality of electrons in graphene as well as carbon nanotubes (CNTs).<sup>20</sup> Without appropriately defined configurations (i.e., zigzag or armchair edges), the conductive channels of GNR-based devices will be irregular.<sup>12</sup>

Linear atomic carbon wires, regarded as extremely narrow GNRs (sub-nanometer width), can be used as a transport channel or as on-chip interconnects for molecular electronic or spintronic nanodevices.<sup>21,22</sup> This choice could bypass the two challenges mentioned above (sub-10-nm and chirality), since atomic carbon chains are atomically thin and not chiral. However, whether these carbon atomic wires are conducting remains an open question.<sup>7,23–25</sup> Several groups have made theoretical predictions on the conductance of carbon atomic wires connected between carbon wire electrodes (sp connection; see Supporting Information, Figure S1a) or CNT or metal electrodes (sp<sup>3</sup> connection; see Supporting Information, Figure S1c,d).<sup>26–34</sup> Lang et al. predicted odd–even atom-number-dependent conductance oscillation of carbon wires; the atomic carbon wire consisting of an odd number of carbon atoms has a large conductance due to its high DOS at the Fermi level.<sup>27</sup> However, Zhou et al. proposed that the conductance of atomic carbon wires consisting of even numbers of carbon atoms is larger than that of the wires consisting of odd numbers of carbon atoms and the conductance oscillation is damped due to charge transfer from electrodes to carbon wires.<sup>28</sup> Besides the conductance, the unique  $I$ – $V$  curve of linear atomic carbon wires has also been widely investigated. Guo and Louie theoretically predicted negative differential resistance (NDR) in carbon wires between metal and capped CNT electrodes,<sup>31,33</sup> which was later observed experimentally.<sup>4</sup> Moreover, the transport of spin current has been studied for zigzag GNR-based spin-electronic devices, since spin-polariza-

tion of zigzag GNRs is well known.<sup>14</sup> Recently, Zeng et al. proposed perfect spin-valve and spin-filter effects in zigzag GNR–carbon chain junctions.<sup>35</sup> Very recently, Furst et al. proposed atomic carbon chains as spin-filters when joining two graphene flakes.<sup>36</sup>

Most theorists conclude that linear atomic carbon wires should have good conductance ( $1–2 G_0$  ( $G_0 = 2e^2/h$ ), where  $e$  and  $h$  are electron charge and Planck's constant, respectively) between either bulk electrodes or nanoelectrodes. However, Yuzvinsky et al. reported their experimental result that the conductance of carbon wires is an order of magnitude lower than theoretically predicted.<sup>4</sup> Ravagnan et al. believed that the electronic properties of sp carbon wires are sensitive to the sp<sup>2</sup> or sp<sup>3</sup> terminations,<sup>37</sup> and Brandbyge et al. also proposed that transport properties depend on the detailed structure of the electrodes.<sup>29</sup> In brief, wires forming ideal molecular junctions are expected to be highly conducting, but smaller conductance was found experimentally. The open question concerns the origin of this discrepancy. Therefore, systematic research on electron transport in carbon chain–GNR systems becomes important.

In this article, we investigate the electron transport properties of carbon wires connected between graphene electrodes with sp<sup>2</sup> bonding at the joint of the molecular junctions (see Supporting Information, Figure S1b). Moreover, some imperfect carbon wires are also studied. In contrast to the sp bonding interface (carbon wire–carbon wire junctions) or sp<sup>3</sup> bonding interface (carbon wire–metal and carbon wire–carbon nanotube junctions), the sp<sup>2</sup> bonding interface (carbon wire–graphene junctions) shows some unique electron transport properties. For example, oxygen impurities, such as the epoxy group (see Figure 1b), in this system dramatically decrease the conductance. Based on this, the experimentally observed low conductance of carbon wires may be due to the epoxy groups.

## Results and Discussion

Geometry optimization was performed for the scattering region (see Figure 1) using a quasi-Newton method<sup>38</sup> until the absolute value of force acting on each atom was  $<0.05$  eV/Å. We also optimized the scattering region using a first-principles method (VASP code)<sup>39</sup> until the force became  $<0.01$  eV/Å. We did not find distinct differences between the results obtained using these two methods. The electron transport calculations were performed using nonequilibrium Green's function method combined with density functional theory within the Landauer formalism implemented in ATK.<sup>29,40</sup> The Perdew–Zunger exchange and correlation functional within the local density approximation is used. The single- $\zeta$  plus polarization (SZP) basis set is used for H atoms, and the double- $\zeta$  plus polarization (DZP) basis set is used for C atoms in order to preserve a correct description of  $\pi$ -conjugated bonds. The energy cutoff is 150 Ry, and a  $k$ -mesh of  $1 \times 1 \times 100$  was used. Three possible structural configurations of carbon wire–graphene junctions

- (17) Ponomarenko, L. A.; Schedin, F.; Katsnelson, M. I.; Yang, R.; Hill, E. W.; Novoselov, K. S.; Geim, A. K. *Science* **2008**, *320*, 356.
- (18) Yan, Q. M.; Huang, B.; Yu, J.; Zheng, F. W.; Zang, J.; Wu, J.; Gu, B.-L.; Liu, F.; Duan, W. H. *Nano Lett.* **2007**, *6*, 1469.
- (19) Standley, B.; Bao, W. Z.; Zhang, H.; Bruck, J.; Lau, C. N.; Bockrath, M. *Nano Lett.* **2008**, *10*, 3345.
- (20) (a) Kurti, J.; Kresse, G.; Kuzmany, H. *Phys. Rev. B* **1998**, *58*, R8869. (b) Kurti, J.; Zolyomi, V.; Kertesz, M.; Sun, G. Y. *New J. Phys.* **2003**, *5*, 125.
- (21) Kim, W. Y.; Choi, Y. C.; Min, S. K.; Cho, Y.; Kim, K. S. *Chem. Soc. Rev.* **2009**, *38*, 2319.
- (22) Ke, S. H.; Yang, W. T.; Baranger, H. U. *Nano Lett.* **2008**, *8*, 3257.
- (23) Ruitenbeek, J. V. *Physics* **2009**, *2*, 42.
- (24) Standley, B.; Bao, W.; Zhang, H.; Bruck, J.; Lau, C. N.; Bockrath, M. *Nano Lett.* **2008**, *8*, 3345.
- (25) Chen, W.; Andreev, A. V.; Bertsch, G. F. *Phys. Rev. B* **2008**, *80*, 085410.
- (26) Tongay, S.; Senger, R. T.; Das, S.; Ciraci, S. *Phys. Rev. Lett.* **2004**, *93*, 136404.
- (27) (a) Lang, N. D.; Avouris, P. *Phys. Rev. Lett.* **1998**, *81*, 3515. (b) Lang, N. D.; Avouris, P. *Phys. Rev. Lett.* **2000**, *84*, 358.
- (28) Zhou, Y. H.; Zheng, X. H.; Xu, Y.; Zeng, Z. Y. *J. Phys.: Condens. Matter* **2008**, *20*, 045225.
- (29) Brandbyge, M.; Mozos, J. L.; Ordejon, P.; Taylor, J.; Stokbro, K. *Phys. Rev. B* **2002**, *65*, 165401.
- (30) Larade, B.; Taylor, J.; Mehrez, H.; Guo, H. *Phys. Rev. B* **2001**, *64*, 075420.
- (31) Kaun, C. C.; Guo, H. *Nano Lett.* **2003**, *3*, 1521.
- (32) Wei, Y. H.; Xu, Y.; Wang, J.; Guo, H. *Phys. Rev. B* **2004**, *70*, 193406.
- (33) Khoo, K. H.; Neaton, J. B.; Son, Y.-W.; Cohen, M. L.; Louie, S. G. *Nano Lett.* **2008**, *8*, 2900.
- (34) Cheraghchi, H.; Esfarjani, K. *Phys. Rev. B* **2008**, *78*, 085123.

- (35) Zeng, M. G.; Shen, L.; Cai, Y. Q.; Sha, Z. D.; Feng, Y. P. *Appl. Phys. Lett.* **2010**, *96*, 042104.
- (36) Furst, J. A.; Brandbyge, M.; Jauho, A. P. <http://arxiv.org>, arXiv:0909.1756.
- (37) Ravagnan, L.; Manini, N.; Cinquanta, E.; Onida, G.; Sangalli, D.; Motta, C.; Devetta, M.; Bordoni, A.; Piseri, P.; Milani, P. *Phys. Rev. Lett.* **2009**, *102*, 245502.
- (38) Press, W. H.; Teukolsky, S. A.; Vetterling, W. T.; Flannery, B. P. *Numerical Recipes*, 3rd ed.; Cambridge University Press: Cambridge, UK, 2007.
- (39) Kresse, G.; Hafner, J. *Phys. Rev. B* **1994**, *49*, 14251.
- (40) Taylor, J.; Guo, H.; Wang, J. *Phys. Rev. B* **2001**, *63*, 121104.

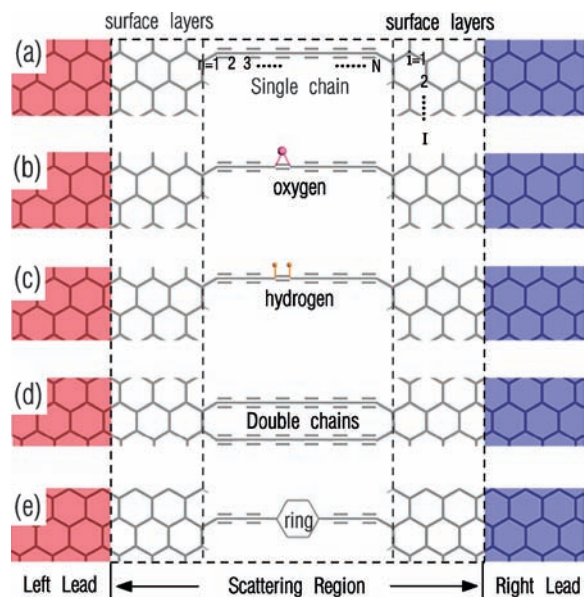


**Figure 1.** Schematic diagrams of two-probe systems. Metallic zigzag graphene nanoribbon electrodes bridged by (a) a perfect linear single-carbon wire (the width of the electrode ( $i$ ) is labeled), (b) a single-carbon wire with oxygen atom adsorption, (c) a single-carbon wire with hydrogen atom adsorption, (d) linear double-carbon wires, and (e) a linear single-carbon wire with a six-membered carbon ring (benzene). In order to properly screen the induced electric field between two electrodes, an adequate number of surface layers is essential. The scattering region is defined as the surface layers combined with the carbon wire system.

(five-, six-, and three-membered rings) are investigated (see Supporting Information, Figure S2). The six-membered ring configuration in S2 is energetically more stable. Note that, after structural optimization, the carbon chain becomes bent due to the  $\sim 120^\circ$  bonding angle at the edge of the six-membered ring. Moreover, the influence of the joint and contact edge and edge-reconstruction on the transport is investigated (see Supporting Information, Figures S2 and S3). Our calculations show that there is no obvious influence on the transport property by changing the connection point and connecting edge, but the transport will be affected by edge-reconstruction. This is because the electronic transport is mainly along the edge states of GNR electrodes. Only a disruption of the edge states, such as edge-reconstruction, suppresses transmission. Therefore, the six-membered ring configuration with the central contact point and hydrogen-passivated GNR electrodes, as shown in Figure S2, is used in our subsequent calculations.

Figure 1 schematically shows the atomic structures used in our calculations. Metallic zigzag GNRs are chosen as the electrodes since armchair GNRs are semiconducting and have poor conductance (see Supporting Information, Figure S4). The inset of Figure 2a shows the effects of the width of the GNR electrodes on conductance of  $C_7$  and  $C_8$ . As can be seen, the width of the GNR electrode does not have an obvious effect on the conductance, due to the fact that only the edge state contributes to transport property of zigzag GNRs. Besides the width of the electrodes, different widths of surface layers (see Figure 1) are also tested in order to investigate the influence of distance between the two electrodes (see Supporting Information, Figure S5). Enough surface layers are essential in order to properly screen the induced electric field between two electrodes separated by a short distance. Our calculations show that the transport property of the carbon chains does not change appreciably when there are four or more surface layers.

Therefore, six electrode layers and four surface layers are used in subsequent calculations. Besides perfect single linear carbon wires consisting of odd or even numbers of carbon atoms (Figure 1a), we also study carbon wires with structural defects, such as wires adsorbed with hydrogen or oxygen and a wire containing a six-membered carbon ring in the middle, as well as double-carbon wires (Figure 1b–e). The cases shown in Figure 1d,e have been observed in experiment with a high probability.<sup>6,7</sup> We focus only on the charge transport property in this work since the spin-polarized calculation produces similar results for the oscillatory conductance.<sup>35</sup>

We optimize the structures of  $C_7$ ,  $C_8$ ,  $C_{15}$ , and  $C_{16}$ . The wires with odd numbers of carbon atoms favor cumulene ( $\cdots C=C=C=C \cdots$ ) (Figure S6a,c), but those consisting of even numbers of carbon atoms prefer polyene ( $\cdots C=C-C=C \cdots$ ) (Figure S6b,d). The values of bond length alternation of short chains are in good agreement with other reported values.<sup>7,26,27,41</sup> The different bond configurations of carbon wires consisting of odd or even numbers of carbon atoms are also evident in their electron density distribution (see Supporting Information, Figure S7).

Based on the optimized structures (scattering region) above, we next calculate the transmission coefficient of carbon wire–graphene junctions with carbon wire length ranging from 3–32. As shown in Figure 2a, the conductance of the carbon wire shows a dampened oscillatory behavior. The atomic carbon wires consisting of odd numbers of carbon atoms have conductance close to  $G_0$ , indicating ballistic electronic transport in these wires, while those consisting of even numbers of carbon atoms have much lower conductance, particularly for short wires. This oscillation has been partially explained in the case of metal electrodes.<sup>27</sup> In a free-standing carbon wire with  $N$  atoms, there are  $(N-1)/2$  fully occupied p orbitals for odd  $N$  and  $(N/2) - 1$  fully occupied p orbitals plus one half-filled p orbital for even  $N$  (see Supporting Information, Figure S8). However, when the wire is in contact with metallic electrodes, it can accept electrons from the electrodes and add a new unoccupied p orbital for odd  $N$  or fill the partially occupied p orbital for even  $N$ . The electronic structure of free carbon wires is modified by the electrodes. Therefore, the molecule–lead interaction may result in the odd–even conductance oscillation.

To further understand the characteristics of this oscillatory behavior, especially the ballistic transport observed in odd-number or long wires, we systematically study the electronic structural modification of the wires by the electrodes. First, the molecule–lead charge transfer is investigated (see Figure 2b). As can be seen, both the total charge transfer from the lead to the wire and the charge transfer per carbon atom show an oscillatory property similar to that exhibited by conductance. Charge transfer from the lead to the molecules affects the conductance of the system. As we know, the molecule–lead coupling is reflected by the electronic structure of the molecule–lead system, which is provided by the DOS at the Fermi level. High DOS leads to a high conductance, and thus the calculated oscillatory behavior of the conductance can be explained by the electronic structure of the molecule–lead system. For example, the DOS of  $C_7$  at the Fermi level is higher than that of  $C_8$  (see Supporting Information, Figure S8). Therefore, the transmission of  $C_7$  at the Fermi level is higher than that of  $C_8$ . It is interesting to note that oscillatory

(41) Kurti, J.; Magyar, C.; Balazs, A.; Rajczy, P. *Synth. Met.* **1995**, *71*, 1865.

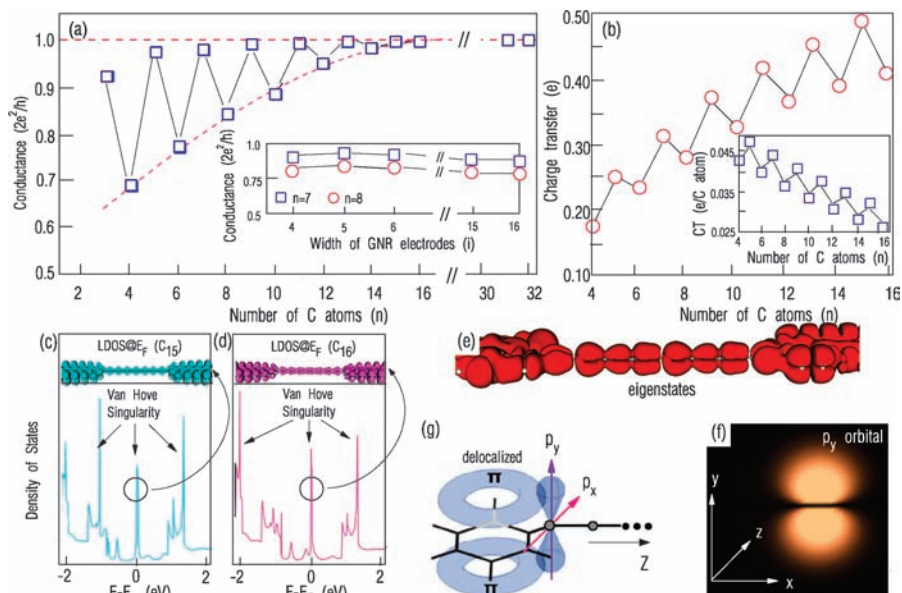


**Figure 2.** (a) Length-dependent conductance oscillation of a single-carbon wire–graphene junction. The inset shows the dependence of conductance on the width of GNR electrodes. (b) Amount of charge transferred as a function of the number of carbon atoms in the wire. The inset shows the amount of charge transferred per carbon atom as a function of the length of the wire. Both of them show an oscillatory property. (c,d) Density of states (DOS) and spatial local density of states (LDOS) of carbon wire–graphene junctions with 15 and 16 carbon atoms. DOS spectrum is discontinuous, with some singularities. The peak at the Fermi level indicates that both  $C_{15}$  and  $C_{16}$  have good conductance and the odd–even effect has disappeared. (e) The eigenstate of a 16-carbon-atom model and (f) the axis view of the eigenstate. (g) Schematic illustration of the transport channel in carbon wire–graphene junctions. It is derived from the overlap of delocalized big  $\pi$  orbitals of GNRs and the  $p_y$  orbital of carbon chains. The  $z$ -axis is along the carbon wire direction.

conductance is seen only in short chains and disappears when the wire becomes long (Figure 2a). When the carbon wires are long enough, the conductance approaches  $\sim 1G_0$ , which is the value of ballistic transport via one eigenchannel. For example, the transmission eigenvalues of both  $C_{15}$  and  $C_{16}$  are close to  $1G_0$  (see Figure 2a). From a physical point of view, a transmission eigenvalue close to 1 means that the incoming wave function is not scattered. This interesting phenomenon indicates that the conductance is essentially not affected by the odd–even effect in carbon wire–graphene junctions if the wire is long enough. This trend can be understood since the effect of the electrode on the electronic structure of a long wire is smaller than that on a short wire, which is also reflected by the DOS at the Fermi level of the molecule–lead system. For example, the DOSs of  $C_{15}$  and  $C_{16}$  structures, including the electrodes, are plotted in Figure 2c,d. In contrast to the continuous DOS of carbon wires between metallic electrodes,<sup>27</sup> some singularities occur in the DOS as in the case of CNTs;<sup>20</sup> especially, a peak occurs at the Fermi level in both  $C_{15}$  and  $C_{16}$ , leading to the corresponding perfect conductance. The fact that both  $C_{15}$  and  $C_{16}$  have peaks at the Fermi level explains why long carbon wires have similar transport properties, independent of the number of carbon atoms. The spatial LDOSs at the Fermi level of  $C_{15}$  and  $C_{16}$  are also plotted in Figure 2c,d, where perfect conductance is suggested in both  $C_{15}$  and  $C_{16}$ . Note that the projected DOSs might be misleading in terms of the conductance due to a cancellation of border zone anomalies.<sup>42</sup> However, this does not apply to our conclusion, since no such cancellation occurs in the GNR–oligomer system.<sup>43</sup>

Next, we discuss why there is only one eigenchannel in wire–graphene junctions, but two in wire–wire and wire–metal

systems. The eigenstates of  $C_{16}$  are shown in Figure 2e, and its axis view is shown in Figure 2f. It can be seen that only the  $p_y$  channel ( $y$  is the direction perpendicular to the graphene plane) is fully open. In general, transmission eigenstates indicate the electronic states that contribute to the conductance. Figure 2g schematically shows that only the  $p_y$  channel of carbon wires overlaps with the delocalized big  $\pi$  orbital of graphene; thus, only the  $p_y$  transport channel contributes to the conductance. As for carbon wire–wire junctions (see Supporting Information, Figure S1a), both  $p_x$  and  $p_y$  orbitals of carbon wires and carbon wire electrodes overlap, since the scattering region and the electrodes are the same. There are also two open channels in wire–metal junctions (see Supporting Information, Figure S1d) due to the Fermi sea of free electrons in metal electrodes.

There was a high probability to form double-atomic carbon wires and a carbon wire with a six-membered carbon ring embedded in the experiments reported by Chuvilin and Jin<sup>6,7</sup> (see the insets of Figure 3a,b). Moreover, as we know, hydrogen and oxygen impurities are the most common defects in experiments. Therefore, besides a single-carbon wire, we also investigate the electron transmission of imperfect carbon wires (see Figure 1b–e). Figure 3 shows their transmission spectra. (Magnified views of Figure 3c,d near the Fermi level are shown in Figure S10 of the Supporting Information.) Surprisingly, except for the oxygen impurity under a low bias, the conductance is independent of all imperfections in the wire structures. The inset of Figure 3d shows that the oxygen atom blocks the transmission eigenstate from one electrode to the other. This is because oxygen atoms act as electron “traps” and form localized states of electrons. Yuzvinsky et al. found the observed conductance of carbon wires to be an order of magnitude lower than predicted under low biases.<sup>4</sup> Ruitenbeek believed that the structure in Yuzvinsky’s experiments was not a perfect carbon wire, and the impurity responds to the low measured conductance.<sup>23</sup> Chen et al. illustrated that the experimentally observed

(42) Cuniberti, G.; Fagas, G.; Richter, K. *Chem. Phys.* **2002**, *465*, 281.

(43) (a) Fagas, G.; Kambili, A.; Elstner, M. *Chem. Phys. Lett.* **2004**, *389*, 268. (b) Fagas, G.; Kambili, A., <http://arxiv.org>, arXiv:cond-mat/0403694.

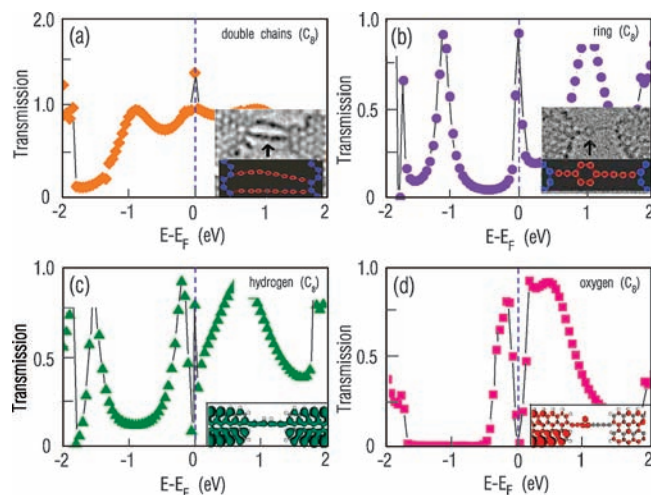


**Figure 3.** Transmission spectra of graphene bridged by double-carbon wires (a), a carbon wire with a six-membered carbon ring (b), a carbon wire with a hydrogen atom adsorbed (c), and a carbon wire with an oxygen atom adsorbed (d). The insets of (a) and (b) (from refs 6 and 7) show experimental observation of double-carbon wires and a carbon wire with a six-membered carbon ring. The insets of (c) and (d) show the spatial LDOS (at the Fermi energy) of a carbon wire with a hydrogen atom adsorbed and an oxygen atom adsorbed. Oxygen atoms, like an electron “trap”, block the transmission eigenstate from the left to the right electrode, resulting in poor conductance. Enlarged versions of (c) and (d) near the Fermi level are plotted in Figure S10 of the Supporting Information. [The inset of (a) is reprinted with permission from ref 6. Copyright 2009 Institute of Physics. The inset of (b) is reprinted with permission from ref 7. Copyright 2009 American Physical Society.]

low conductance (off-state) is due to a small number of carbon atoms in a different metastable state.<sup>25</sup> However, based on our calculations, the epoxy group (oxygen impurity) may be an origin of low conductance of the carbon wires observed experimentally. Note that the specific conductance of double-carbon wires ( $1.47G_0$ ) is not exactly twice the value of a single-carbon wire ( $1.0G_0$ ). This is due to overlapping of the electron clouds of the two wires (see Supporting Information, Figure S7e).

We show in Figure 4 the  $I$ – $V$  curve of both perfect single-carbon wires and imperfect wires, calculated from

$$I = G_0 \int T(E, V_b) [f_l(E) - f_r(E)] dE \quad (1)$$

where  $f_{l(r)}(E)$  are the Fermi distribution functions at left (right) electrode, respectively.  $T(E, V_b)$  is the transmission coefficient at energy  $E$  and bias voltage  $V_b$ . The  $I$ – $V$  curve shows that the double-atomic carbon wire system exhibits NDR,<sup>31,33,44,45</sup> with dips in the current occurring between 1.2 and 1.8 eV for the wires consisting of odd numbers of carbon atoms and between 1.4 and 2.0 eV for the wires consisting of even numbers of carbon atoms. In order to understand the physical origin of the NDR in the double-carbon wire system, the transmission spectra at four typical biases are shown in Figure 4c–f for the seven-carbon atom junction. As we can see, the current within the bias window around the Fermi level is mainly contributed by two peaks (P1 and P2). Compared to the case of 0.8 eV bias, the two transmission peaks at 1.2 eV bias are significantly enhanced, resulting in a dramatic increase in the current.

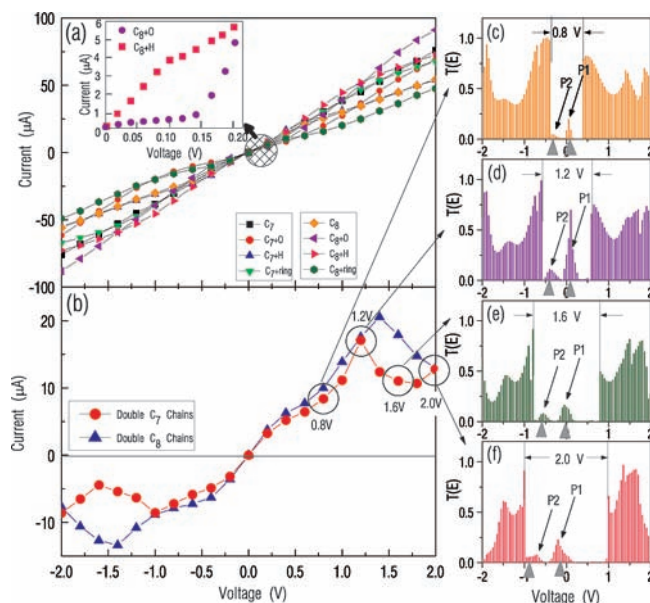


**Figure 4.** (a)  $I$ – $V$  curves of GNR bridged by carbon wires (seven and eight carbon atoms) with a six-membered carbon ring, a hydrogen atom, and an oxygen atom. The inset shows the  $I$ – $V$  characteristics of the  $C_6$  wire with an oxygen and a hydrogen atom under a low bias voltage. As can be seen,  $C_8 + H$  shows a metallic property, but  $C_8 + O$  shows a semiconducting property. Therefore, the oxygen atoms suppress the conductance under a low bias. (b)  $I$ – $V$  characteristics of double-carbon wire–graphene junctions (seven and eight carbon atoms). It shows a negative differential resistance effect above 1.2 V. (c)–(f) Transmission spectra of double  $C_7$  wires under a bias of 0.8, 1.2, 1.6, and 2.0 eV, respectively. The arrows in the bias window point to two transmission peaks that make the main contribution to the current. The energy level of these two transmission peaks is consistent with the molecular orbitals of carbon wires. The gray triangles in (c)–(f) indicate the molecular projected self-consistent Hamiltonian near the Fermi level. Two MPSH eigenvalues around the Fermi level give rise to two peaks (P1, P2) in the bias window since they are affected by the frontier molecular orbitals. Due to the charge transfer under biases, the localized charge at the point contacts (between electrodes and carbon wires) generates Schottky-like barriers. The height of the barriers is around the value of the bias voltage. Therefore, most transmission in the bias window is blocked, except for two broadened molecular orbitals near the Fermi level. The Fermi level is set to zero.

However, the two transmission peaks in the bias window decrease steadily with continuous increasing applied bias to 1.6 eV, and this decrease causes a drop in current. The current then increases again with the increase of two transmission peaks, as demonstrated in Figure 4f for 2.0 eV bias, resulting in the NDR effect. Since the energy level of transmission peaks is consistent with the molecular orbitals of carbon wires, we calculate the molecular projected self-consistent Hamiltonian (MPSH) of the carbon wires. Two MPSH eigenvalues around the Fermi level, labeled by gray triangles in Figure 4c–f, give rise to two transmission peaks (P1, P2) within the bias window since they are affected by the frontier molecular orbitals. Due to the effect of electrodes, the two molecular orbitals are broadened, resulting in two broad transmission peaks within the bias window. Moreover, the localized charge at the point contacts generates Schottky-like barriers. The height of the barriers is around the value of bias voltage. Therefore, most transmission in the bias window is blocked, except for two broadened molecular orbitals near the Fermi level.

## Conclusion

In conclusion, we have investigated electron transport properties of carbon wire–graphene junctions. It is found that

(44) Zhou, L. P.; Yang, S.-W.; Ng, M.-F.; Sullivan, M. B.; Tan, V. B. C.; Shen, L. *J. Am. Chem. Soc.* **2008**, *130*, 4023.

(45) Liu, R.; Ke, S. H.; Baranger, H. U.; Yang, W. T. *J. Am. Chem. Soc.* **2006**, *128*, 6274.

conductance in the atomic wires can be ballistic, independent of structural defects such as structural distortion, adsorption of impurities, etc. This information suggests that it is unnecessary to get a perfect single-carbon wire experimentally in order to obtain perfect conductance in devices. Some imperfect wires, such as double-atomic wires or a single wire with a six-membered carbon ring, also exhibit perfect conductance. Moreover, introduction of hydrogen impurities in experiment will not affect the conductance of the system, but oxygen impurities can strongly reduce it under a low bias. Finally, the negative differential resistance effect is found in double-atomic carbon wires. With these unique properties, carbon wire–graphene junctions hold promise for use in molecular devices, quantum dot devices, and carbon-based field-effect transistors.

**Acknowledgment.** The authors thank Dr. V. Ligatchev, Dr. B. Xu, and Dr. Y. H. Lu for their insightful discussions.

**Supporting Information Available:** Different configurations of carbon wire–electrode junctions and carbon wire–graphene junctions; connecting edges; edge shapes; distance between two electrodes; optimized structures of  $C_7$ ,  $C_8$ ,  $C_{15}$ , and  $C_{16}$  carbon chains; charge density of carbon wire–graphene junctions; molecular orbital modification by coupling with electrodes; DOSs of  $C_7$  and  $C_8$  at the Fermi level; and enlarged transmission spectra of H- and O-adsorbed  $C_8$  near  $E_F$ . This material is available free of charge via the Internet at <http://pubs.acs.org>.

JA909531C